ChemCatChem

Supporting Information

Manganese Oxide as an Inorganic Catalyst for the Oxygen Evolution Reaction Studied by X-Ray Photoelectron and Operando Raman Spectroscopy

Hannes Radinger,* Paula Connor, Robert Stark, Wolfram Jaegermann, and Bernhard Kaiser*

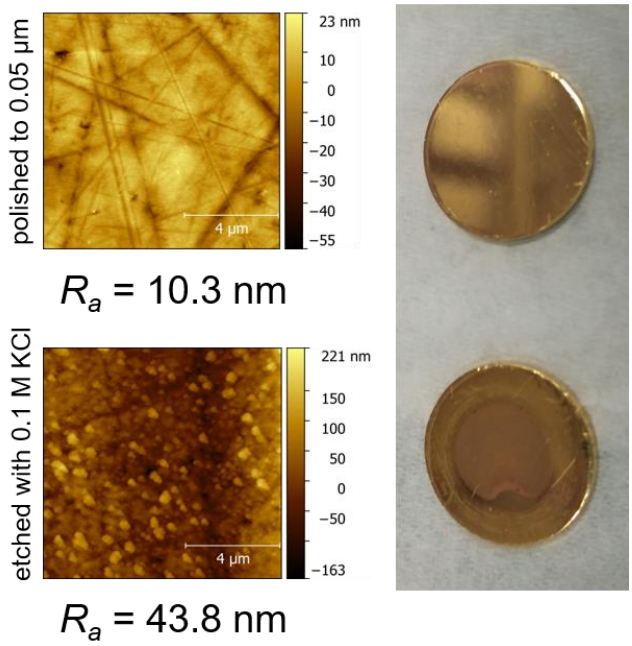

Figure S1. Left panel: AFM images of the polished and the etched gold substrate with the average roughness based on three images; right panel: pictures of the gold coins before and after the KCl treatment.

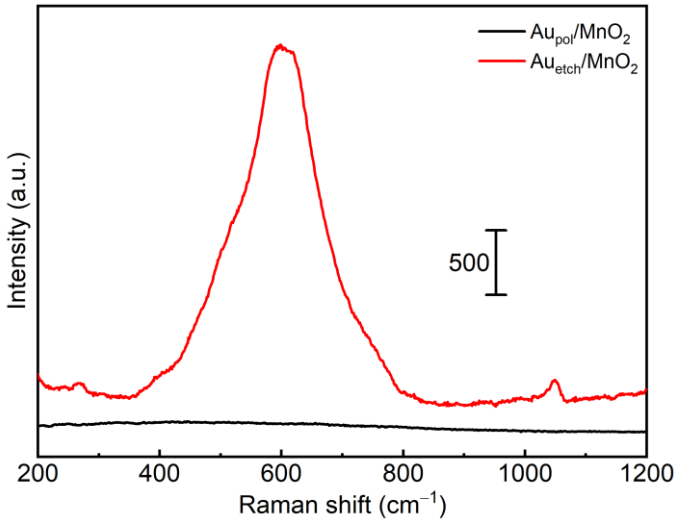

Figure S2. Raman spectra of a sputter deposited MnO_2 film on a polished and roughened gold substrate to demonstrate the effect of the surface enhancement.

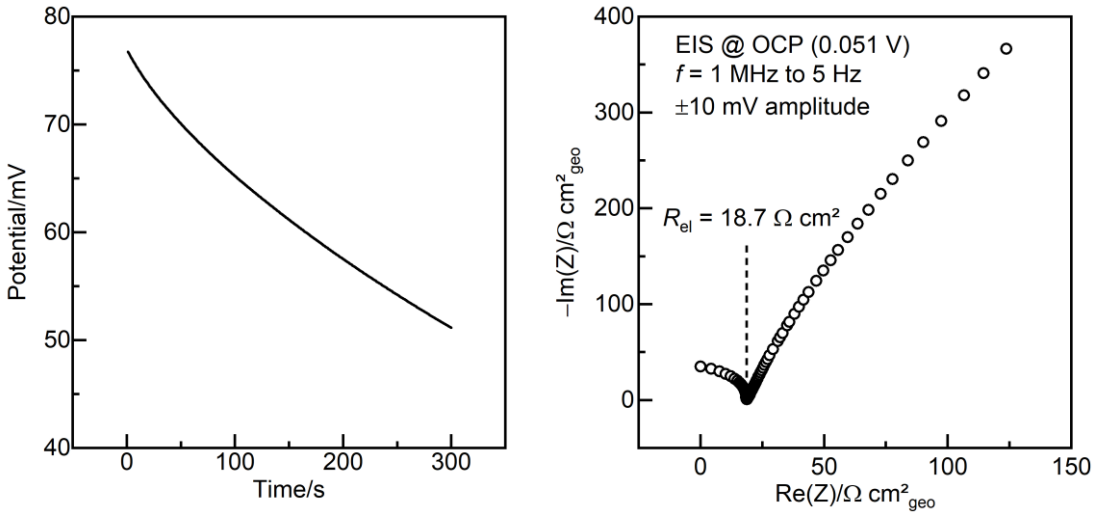

Figure S3. Procedure for the determination of the electrolytic resistance. The OCP is recorded for 10 min and the respective value at the end used to measure EIS with a voltage amplitude of ±10 mV. The real impedance value closest to zero imaginary impedance (*e.g.* 18.7 **Ω** cm²) is used as electrolytic resistance and to *iR* correct the voltammetry results according to E(corrected) = E(measured) – i(measured) × R_{el}.

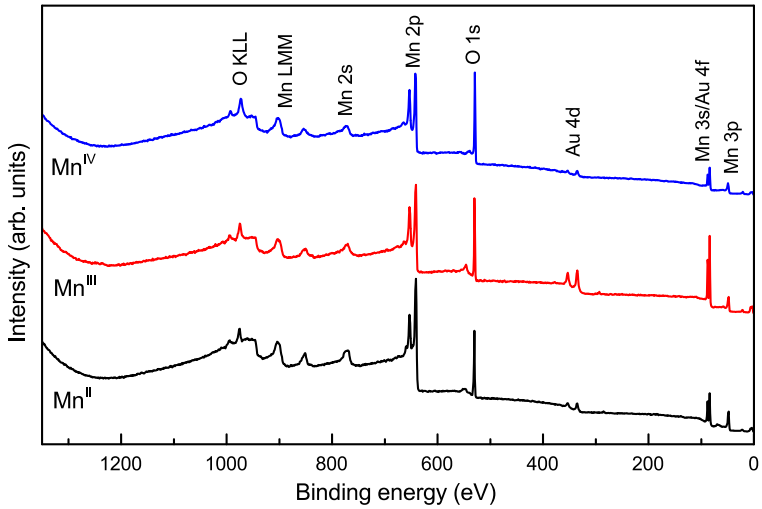

Figure S4. XP survey spectra of reactively magnetron sputtered MnO_x on gold. All peaks in the spectra are assigned to manganese, oxygen, and gold.

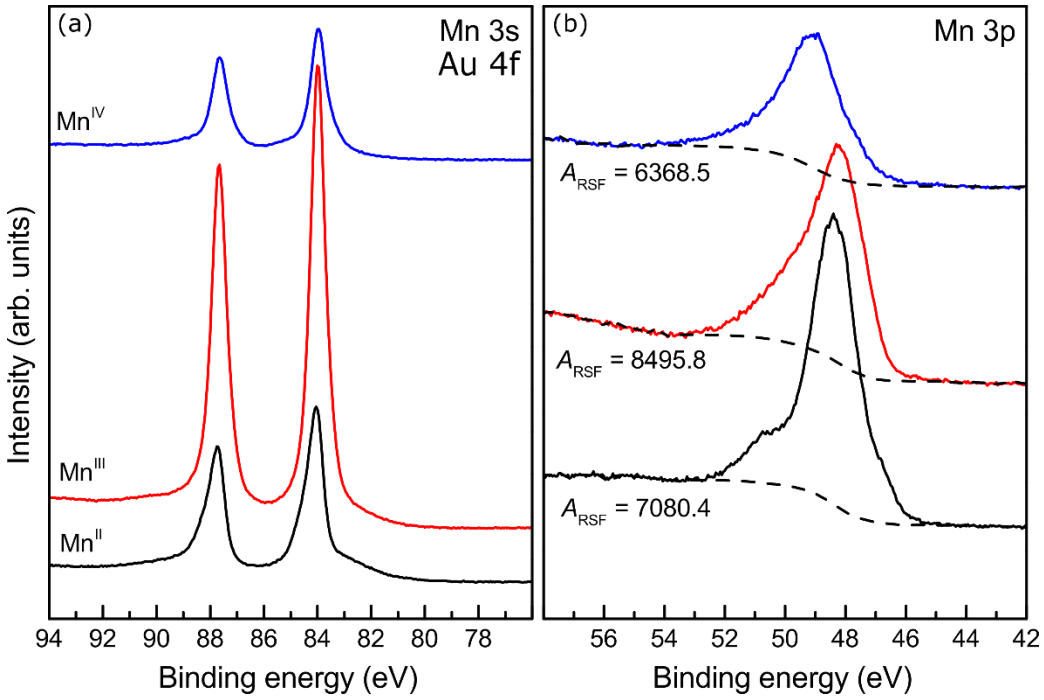

Figure S5. XP detail spectra of reactively magnetron sputtered MnO_x on gold. (a) The figure presents the overlapping Mn 3s and Au 4f region, which is dominated by the Au 4f peaks. (b) The Mn 3p region, subtracted with a Shirley BG. The area was calculated with a relative sensitivity factor (RSF) of 1.423.

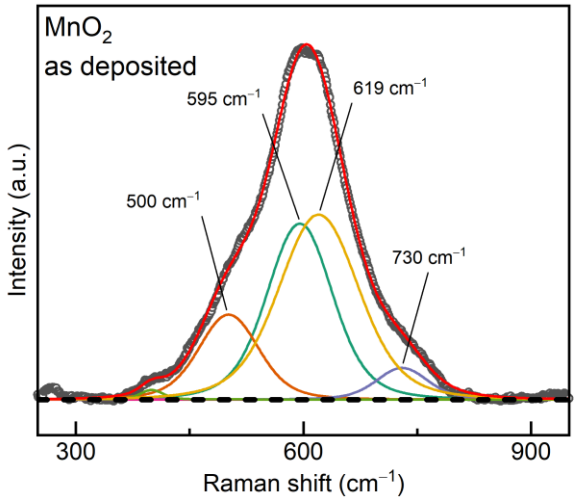

Figure S6. Deconvoluted SER spectrum of MnO_2 directly after the sputter deposition.

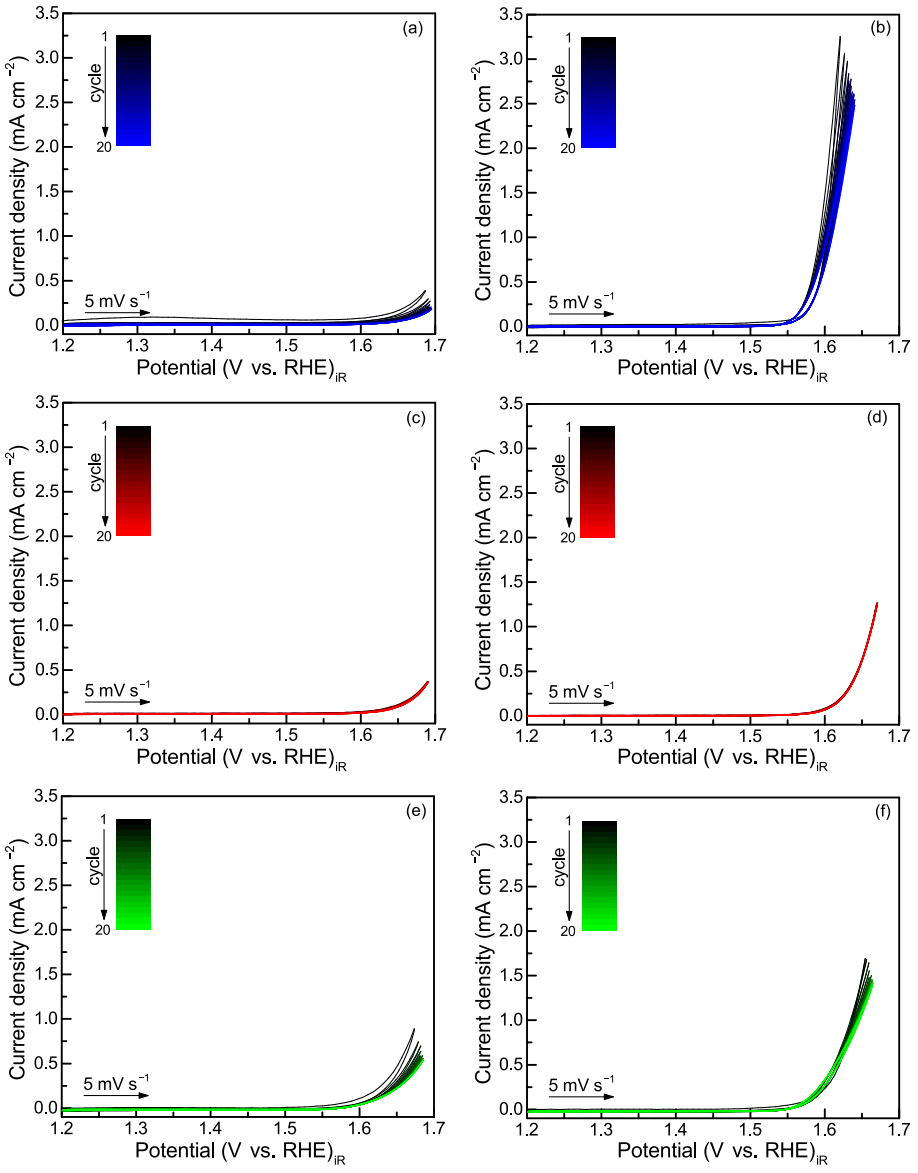

Figure S7. First (left panel) and second activation (right panel) process of Mn^{II} (a, b), Mn^{III} (c, d), and Mn^{IV} (e, f). Samples were cycled 20 times from 1.2 to 1.7 V *vs.* RHE in 0.1 M KOH. Activity degradation is indicated by the color map.

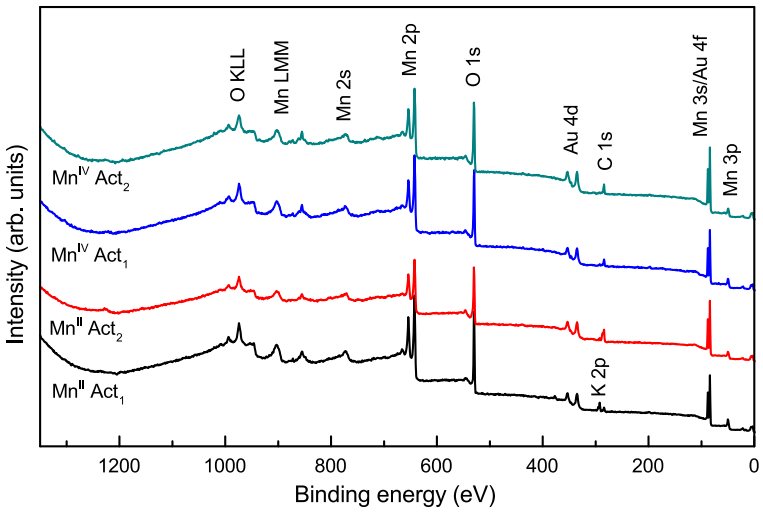

Figure S8. XP survey spectra of MnO_x after activation (Act_1) and reactivation (Act_2). All peaks are assigned to manganese, oxygen, gold, carbon, and potassium from the KOH electrolyte.

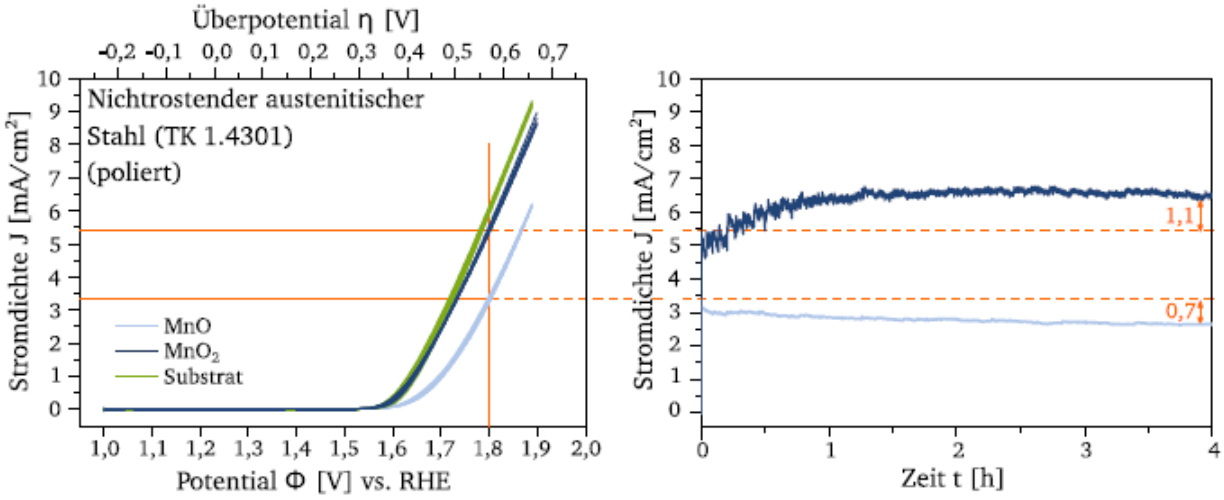

Figure S9. Long-term stability measurements of MnO and MnO_2 on stainless steel (1.4301).

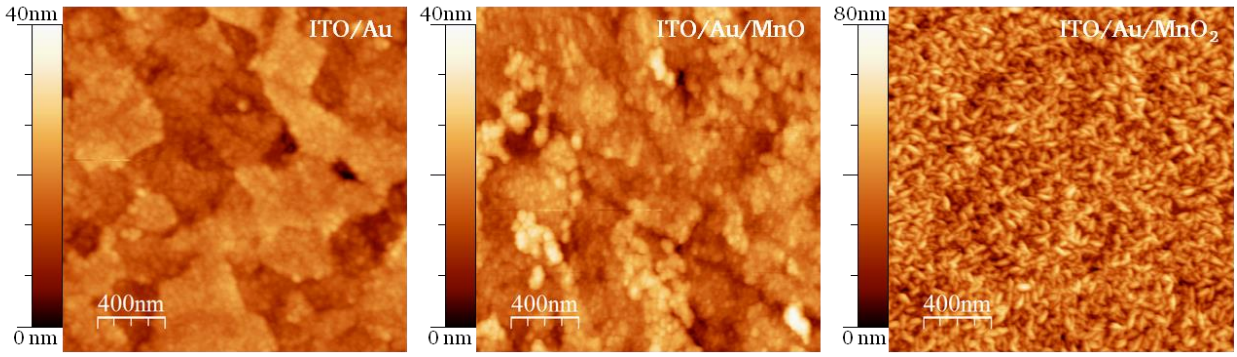

Figure S10. AFM pictures of the substrate ITO/Au (1 cm^2_{geo} ~ 1.013 cm^2) as well as of the samples MnO and MnO_2 on ITO/Au (2 × 2 μm^2 each). The substrate platelets are still visible under the MnO film (~1.028 cm^2). Additionally, ball-like agglomerates can be detected. In contrast, MnO2 (~1.374 cm^2) reveals a dendrite-like structure.[3]

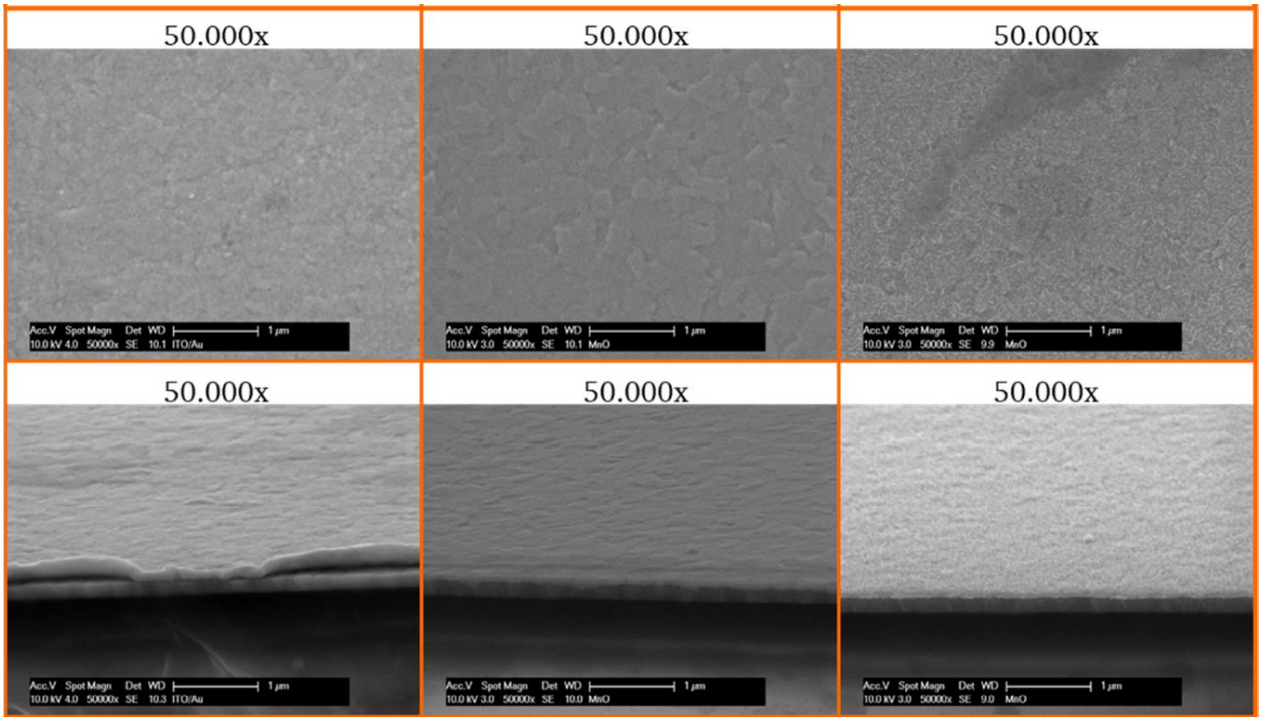

Figure S11. SEM images of the ITO/Au substrate and the MnO and MnO2 samples on ITO/Au. The pictures were taken with 10 kV excitation energy. The results are consistent with the AFM images. The underlying substrate is visible beneath the manganese oxides. Regions with varying structure can be seen.

Table S1. Kinetic parameters of freshly deposited MnO_x in 0.1 M KOH.

Sample	OER onset [V]	η at 5 mA cm^{-2} [mV]	Tafel slope [mV dec^{-1}]
Mn^{II}	1.62	550	88
Mn^{III}	1.64	540	77
Mn^{IV}	1.60	490	62

Table S2. Kinetic parameters of MnO_x obtained by LSV after Act_1 and Act_2.

	OER onset [V]		η at 5 mA cm^{-2} [mV]		Tafel slope [mV dec^{-1}]	
Sample	Act_1	Act_2	Act_1	Act_2	Act_1	Act_2
Mn^{II}	1.64	1.57	540	430	79	44
Mn^{III}	1.63	1.60	540	530	82	51
Mn^{IV}	1.60	1.57	540	500	77	73